

## Supporting Information

### Non-aqueous procedure to aminogroup bearing nanostructured organic-inorganic hybrid materials

Mandy Göring, Andreas Seifert, Katja Schreiter, Philipp Müller<sup>#</sup>, and Stefan Spange\*

Department of Polymer Chemistry, Institute of Chemistry, Technische Universität Chemnitz, Strasse der Nationen 62, D-09111 Chemnitz, Germany, e-mail: stefan.spange@chemie.tu-chemnitz.de

<sup>#</sup>BASF SE, Carl-Bosch Straße 38, 67056 Ludwigshafen (Deutschland)

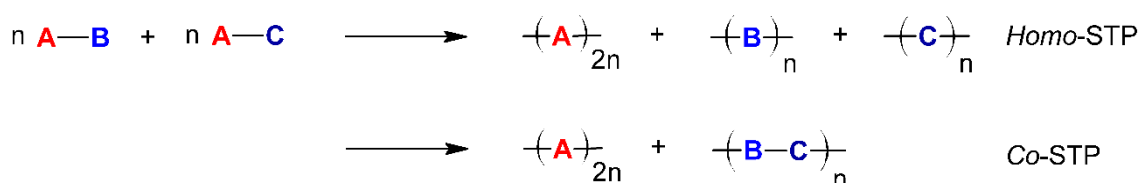


Figure 1: Theoretical scenarios of simultaneous twin polymerization of two twin monomers with the same organic unit A and different inorganic units B and C

### Experimental

#### General Information:

All materials were purchased from commercial suppliers. All solvents were dried with appropriate drying agents and freshly distilled before usage.

Solid state NMR spectra were collected at 9.4 T on a Bruker Avance 400 spectrometer equipped with double tuned probes capable of MAS (magic angle spinning). <sup>13</sup>C-{<sup>1</sup>H}-CP MAS-NMR spectra were measured at 100.6 MHz in 3.2 mm standard zirconium oxide rotors (BRUKER) spinning at 15 kHz. Cross polarization with a contact time of 3 ms was used to enhance the sensitivity. The recycle delay was 6 s. Spectra were referenced externally to tetramethylsilane (TMS) as well as to adamantane as secondary standard (38.48 ppm for <sup>13</sup>C). <sup>29</sup>Si-{<sup>1</sup>H}-CP-MAS-NMR spectroscopy was performed at 79.5 MHz using 3.2 mm rotors spinning at 12 kHz. The contact time was 3 ms and the recycle delay 6 s. Shifts were referenced externally to tetramethylsilane (0 ppm) with the secondary standard being

tetrakis(trimethylsilyl)silane (-9.8, -135.2 ppm). All spectra were collected with  $^1\text{H}$  decoupling using a TPPM pulse sequence.

The HAADF-TEM images were recorded with a Technai G2-F-20ST with HAADF-STEM-detector (Department of Material Physics & Analytics BASF SE under the leadership of Dr. P. Müller). The samples were prepared by ultramicrotomy.

The DSC measurements were performed by a DSC 1 (Mettler Toledo) in 40  $\mu\text{l}$  aluminum pan and a  $\text{N}_2$ -flow of 50 ml/min.

TGA measurements were performed by a Thermogravimetric Analyzer 7 (Perkin Elmer; Prof. Dr. W. Goedel, Physikalische Chemie, TU Chemnitz). The samples were measured under air atmosphere, with a heating rate of 10 K/min from 30-800  $^\circ\text{C}$ .

The ATR FTIR-spectra were recorded with a FTS 165 spectrometer (BioRad). A Golden Gate-single reflection-ATR-stage (L.O.T. Oriel GmbH) was used. The powdered samples were pressed against the detection system with a sapphire stamp (5 bar).

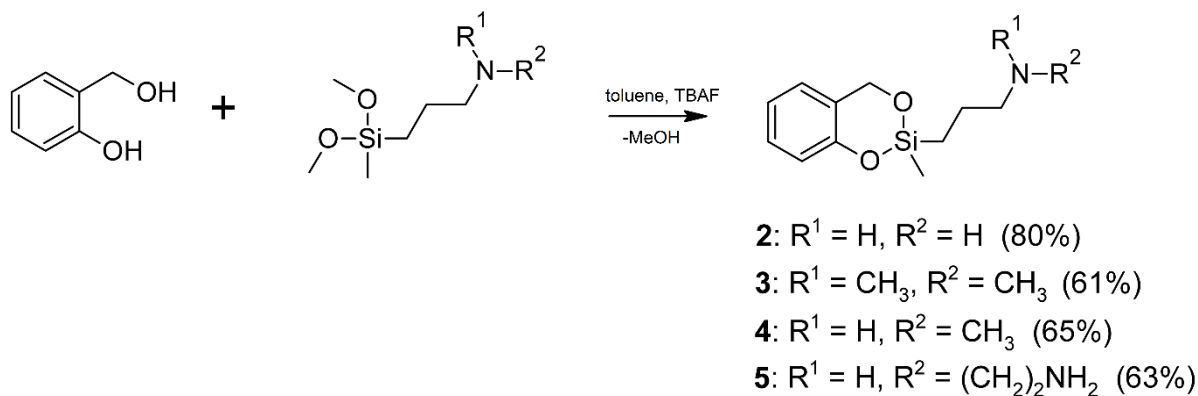
The elemental analysis were carried out with a Vario EI (Elementaranalysensysteme GmbH) (Prof. Dr. Banert, Department organic chemistry, Technische Universität Chemnitz).

### **Synthesis information:**

The established twin monomer **1**, 2,2'-Spirobi[4*H*-1,3,2]-benzodioxasiline was synthesized according to the literature<sup>1</sup>.

### General procedure for synthesis of the monomers **2**, **3**, **4** and **5**

0.05 mL tetra-*n*-butylammonium fluoride (1M in THF) was added into a solution of 0.08 mol salicylic alcohol in 60 ml toluene at 80  $^\circ\text{C}$  under argon atmosphere. Then, 0.08 mol of the respective dimethoxysilane component (0.08 mol) were dropped into the solution over a time period of 15 min. The methanol/toluene azeotropic mixture was removed under reduced pressure. After removal toluene completely, the residual was heated up with hexane. After cooling the solution, the supernatant was decanted from viscous oligomeric by-products. The clear product was distilled at 0.2 mbar.



*Scheme 1. Amino group modified twin-monomers which has been studied in this work for the simultaneous twin-polymerization*

**2-(3-Amino-*n*-propyl)-2-methyl-4*H*-1,3,2-benzodioxasilin (2)**

Yield: 80 %;

bp.: 140°C (0.2 mbar);

<sup>1</sup>H NMR (400 MHz, CDCl<sub>3</sub>, δ): 7.12 – 7.11 (m, 1H, Ar H), 6.99 – 6.82 (m, 3H; Ar H), 4.89 (2d, 4H; CH<sub>2</sub>-O-Si), 2.64 (t, 2H, CH<sub>2</sub>-NH<sub>2</sub>), 1.53 (qi, 2H, CH<sub>2</sub>-CH<sub>2</sub>-CH<sub>2</sub>), 1.23 (s, broad, 2 H, NH<sub>2</sub>) 0.75 (t, 2H, Si-CH<sub>2</sub>), 0.29 (s, 3H, CH<sub>3</sub>);

<sup>13</sup>C NMR (100 MHz, CDCl<sub>3</sub>, δ): 153.2 (Ar C), 128.6 (Ar C), 126.3 (Ar C), 125.8 (Ar C), 120.57 (Ar C), 118.9 (Ar C), 63.7 (CH<sub>2</sub>-O -Si), 44.2 (CH<sub>2</sub>-NH<sub>2</sub>), 26.1 (CH<sub>2</sub>-CH<sub>2</sub>-CH<sub>2</sub>), 12.1 (Si-CH<sub>2</sub>), -2.5 (CH<sub>3</sub>);

<sup>29</sup>Si NMR (CDCl<sub>3</sub>, TMS, δ): -0.296 ppm

IR (ATR-FTIR): ν = 3366, 3281 (w; ν(NH)), 3048 (w, ν<sub>as</sub>(CH<sub>2</sub>)), 2924, 2847 (m, ν<sub>s</sub>(CH<sub>2</sub>)), 1603, 1580 (m, ν(C=C)), 1485, 1458 (s, δ(CH<sub>2</sub>)), 1256 (s, δ(CH<sub>3</sub>)), 1055 (s, ν(SiOC)), 1028 (s, ν(CN)), 787 (s, ν(SiC)), 754 (s, δ(CH));

MS (ESI) *m/z*: [M + H]<sup>+</sup> calcd for C<sub>11</sub>H<sub>17</sub>NO<sub>2</sub>Si, 224.1101; found, 224.1148;

Anal. calcd for C<sub>11</sub>H<sub>17</sub>NO<sub>2</sub>Si: C 59.16, H 7.67, N 6.27; found: C 57.74, H 7.88 N 6.47.

**2-(*N,N*-Dimethyl-3-amino-*n*-propyl)-2-methyl-4*H*-1,3,2-benzodioxasilin (3)**

Yield: 61 %;

bp.: 150 °C (0.2 mbar);

<sup>1</sup>H NMR (400 MHz, CDCl<sub>3</sub>, δ): 7.18 – 7.14 (m, 1H, Ar H), 6.90 – 6.86 (m, 3H; Ar H), 4.92 (2d, 4H; CH<sub>2</sub>-O-Si), 2.23 (m, 2H, CH<sub>2</sub>-NH<sub>2</sub>), 2.17 (s, 6H, N-CH<sub>3</sub>), 1.57 (m, 2H, CH<sub>2</sub>-CH<sub>2</sub>-CH<sub>2</sub>), 0.77 (t, 2H, Si-CH<sub>2</sub>), 0.30 (s, 3H, CH<sub>3</sub>);

<sup>13</sup>C NMR (100 MHz, CDCl<sub>3</sub>, δ): 153.1 (Ar C), 128.8 (Ar C), 126.9 (Ar C), 126.0 (Ar C), 120.8 (Ar C), 119.1 (Ar C), 63.9 (CH<sub>2</sub>-O-Si), 62.2 (N-CH<sub>3</sub>) 45.2 (CH<sub>2</sub>-NH<sub>2</sub>), 20.1 (CH<sub>2</sub>-CH<sub>2</sub>-CH<sub>2</sub>), 12.8 (Si-CH<sub>2</sub>), -2.9 (CH<sub>3</sub>);

<sup>29</sup>Si NMR (CDCl<sub>3</sub>, TMS, δ): 2.775 ppm

IR (ATR-FTIR):  $\nu = 3069$  (w,  $\nu_{\text{as}}(\text{CH}_2)$ ),  $2855$  (m, br,  $\nu_{\text{s}}(\text{CH}_2)$ ),  $1605$ ,  $1582$  (m,  $\nu(\text{C}=\text{C})$ ),  $1485$ ,  $1456$  (s,  $\delta(\text{CH}_2)$ ),  $1255$  (s,  $\delta(\text{CH}_3)$ ),  $1059$  (s,  $\nu(\text{SiOC})$ ),  $1030$  (s,  $\nu(\text{CN})$ ),  $800$  (s,  $\nu(\text{SiC})$ ),  $750$  (s,  $\delta(\text{CH})$ );

MS (ESI)  $m/z$ :  $[\text{M} + \text{H}]^+$  calcd for  $\text{C}_{13}\text{H}_{21}\text{NO}_2\text{Si}$ , 252.1414; found, 252.1415;

Anal. calcd for  $\text{C}_{11}\text{H}_{17}\text{NO}_2\text{Si}$ : C 62.11, H 8.42, N 5.57; found: C 59.32, H 8.36, N 5.04.

#### 2-(N-methyl-3-amino-*n*-propyl)-2-methyl-4*H*-1,3,2-benzodioxasilin (4)

Yield: 65 %

bp.: 150 °C (0.2 mbar)

$^1\text{H}$  NMR (400 MHz,  $\text{CDCl}_3$ ,  $\delta$ ): 7.18 – 7.15 (m, 1H, Ar H), 6.96 – 6.86 (m, 3H; Ar H), 4.91 (2d, 4H;  $\text{CH}_2\text{-O-Si}$ ), 2.55 (m, 2H,  $\text{CH}_2\text{-NH}_2$ ), 2.39 (s, 3H, N- $\text{CH}_3$ ), 2.0 (s, broad, 1H, NH) 1.60 (m, 2H,  $\text{CH}_2\text{-CH}_2\text{-CH}_2$ ), 0.79 (t, 2H, Si- $\text{CH}_2$ ), 0.30 (s, 3H,  $\text{CH}_3$ );

$^{13}\text{C}$  NMR (100 MHz,  $\text{CDCl}_3$ ,  $\delta$ ): 153.1 (Ar C), 128.8 (Ar C), 126.9 (Ar C), 126.0 (Ar C), 120.8 (Ar C), 119.1 (Ar C), 63.9 ( $\text{CH}_2\text{-O-Si}$ ), 62.2 (N- $\text{CH}_3$ ) 45.2 ( $\text{CH}_2\text{-NH}_2$ ), 20.1 ( $\text{CH}_2\text{-CH}_2\text{-CH}_2$ ), 12.8 (Si- $\text{CH}_2$ ), -2.9 ( $\text{CH}_3$ );

$^{29}\text{Si}$  NMR ( $\text{CDCl}_3$ , TMS,  $\delta$ ): - 3.045 ppm

IR (ATR-FTIR):  $\nu = 3307$  (w;  $\nu(\text{NH})$ ),  $3067$  (w,  $\nu_{\text{as}}(\text{CH}_2)$ ),  $2867$  (m, br,  $\nu_{\text{s}}(\text{CH}_2)$ ),  $1603$ ,  $1580$  (m,  $\nu(\text{C}=\text{C})$ ),  $1485$ ,  $1459$  (s,  $\delta(\text{CH}_2)$ ),  $1255$  (s,  $\delta(\text{CH}_3)$ ),  $1059$  (s,  $\nu(\text{SiOC})$ ),  $1028$  (s,  $\nu(\text{CN})$ ),  $797$  (s,  $\nu(\text{SiC})$ ),  $752$  (s,  $\delta(\text{CH})$ );

MS (ESI)  $m/z$ :  $[\text{M} + \text{H}]^+$  calcd for  $\text{C}_{12}\text{H}_{19}\text{NO}_2\text{Si}$ , 238.1258; found, 238.1266;

Anal. calcd for  $\text{C}_{12}\text{H}_{19}\text{NO}_2\text{Si}$ : C 60.73, H 8.07, N 5.89; found: C 59.53, H 8.14, N 5.72.

#### 2-(N-(2-Aminoethyl)-3-Amino-*n*-propyl)-2-methyl-4*H*-1,3,2-benzodioxasilin (5)

Yield: 63 %

bp.: 150 °C (0.2 mbar);

$^1\text{H}$  NMR (400 MHz,  $\text{CDCl}_3$ ,  $\delta$ ): 7.18 – 7.15 (m, 1H, Ar H), 6.98 – 6.86 (m, 3H; Ar H), 4.91 (2d, 4H;  $\text{CH}_2\text{-O-Si}$ ), 2.80 – 2.70 (m, 2H,  $\text{CH}_2\text{-NH}$ ), 2.65 -2.56 (m, 4H,  $\text{CH}_2\text{-NH-CH}_2$ ), 1.71 (s, broad, 3H, NH  $\text{NH}_2$ ) 1.61 (m, 2H,  $\text{CH}_2\text{-CH}_2\text{-CH}_2$ ), 0.79 (t, 2H, Si- $\text{CH}_2$ ), 0.30 (s, 3H,  $\text{CH}_3$ );

$^{13}\text{C}$  NMR (100 MHz,  $\text{CDCl}_3$ ,  $\delta$ ): 153.1 (Ar C), 128.7 (Ar C), 126.9 (Ar C), 125.9 (Ar C), 120.7 (Ar C), 118.9 (Ar C), 63.8 ( $\text{CH}_2$ ) 52.0 ( $\text{CH}_2\text{-NH-CH}_2$ ), 41.4 ( $\text{CH}_2\text{-NH}_2$ ), 22.6 ( $\text{CH}_2\text{-CH}_2\text{-CH}_2$ ), 12.6 (Si- $\text{CH}_2$ ), -2.8 ( $\text{CH}_3$ );

$^{29}\text{Si}$  NMR ( $\text{CDCl}_3$ , TMS,  $\delta$ ): 1.201

IR (ATR-FTIR):  $\nu = 3353$ ,  $3287$  (w;  $\nu(\text{NH})$ ),  $3046$  (w,  $\nu_{\text{as}}(\text{CH}_2)$ ),  $2930$ ,  $2859$  (m, br,  $\nu_{\text{s}}(\text{CH}_2)$ ),  $1597$  (m,  $\nu(\text{C}=\text{C})$ ),  $1485$ ,  $1454$  (s,  $\delta(\text{CH}_2)$ ),  $1252$  (s,  $\delta(\text{CH}_3)$ ),  $1057$  (s,  $\nu(\text{SiOC})$ ),  $1028$  (s,  $\nu(\text{CN})$ ),  $797$  (s,  $\nu(\text{SiC})$ ),  $752$  (s,  $\delta(\text{CH})$ );

MS (ESI)  $m/z$ :  $[\text{M} + \text{H}]^+$  calcd for  $\text{C}_{13}\text{H}_{22}\text{N}_2\text{O}_2\text{Si}$ , 267.1523; found, 267.1537;

Anal. calcd for  $\text{C}_{13}\text{H}_{22}\text{N}_2\text{O}_2\text{Si}$ : C 58.62, H 8.33, N 10.51; found: C 58.16, H 8.408, N 9.94.

### General procedure for the synthesis of the hybrid materials

The nanocomposites were synthesized in melt. The desired ratio of monomer **1** and **2**, **3**, **4** or **5** is heated up to 80 °C under argon atmosphere to form a homogenous melt. Then the mixture was heated until a monolith is formed. The experimental information and a macroscopic photographs of the hybrid materials are shown in table 1.

Table 1. Experimental settings for the fabrication of hybrid materials.

Run	monomer A	monomer B	ratio A : B	temperature [°C]	photograph
P2	1	2	50 : 50	120	
P3	1	3	50 : 50	120	
P4	1	4	50 : 50	120	
P5	1	5	50 : 50	120	
P2_1	1	2	95 : 05	180	
P2_2	1	2	85 : 15	180	
P2_3	1	2	50 : 50	180	
P2_4	1	2	15 : 85	180	
P2_5	-	2	00 : 100	220	

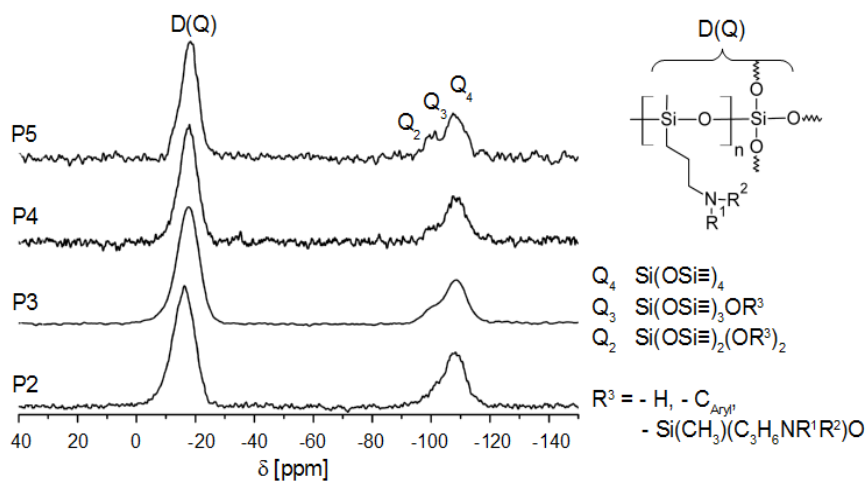


Figure 2.  $^{29}\text{Si}\{-^1\text{H}\}$ -CP-MAS-NMR of samples P2-P5

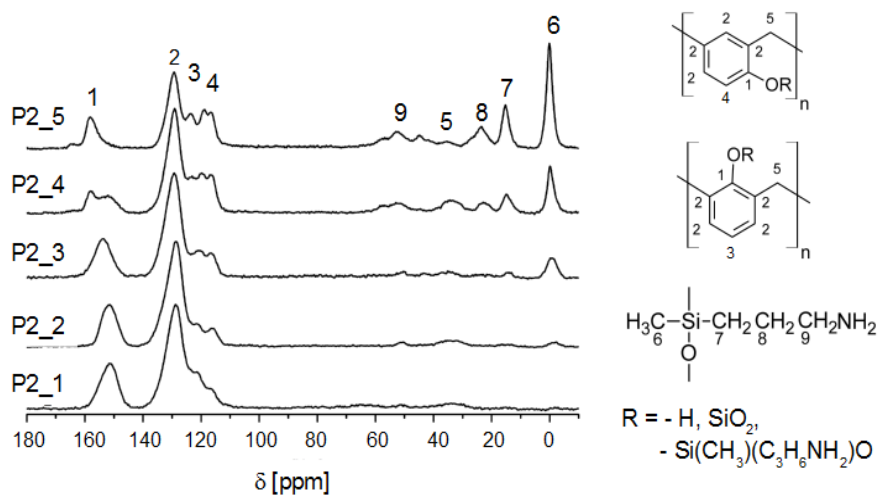
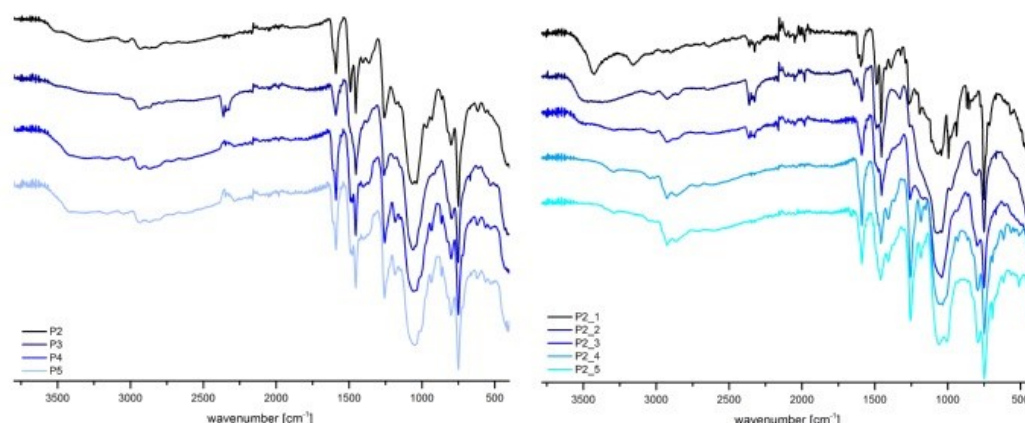


Figure 3.  $^{13}\text{C}\{-^1\text{H}\}$ -CP-MAS-NMR of samples P2\_1-P2\_5

## IR-Spectroscopy of the hybrid materials



*Figure 4. ATR-FTIR-spectra of the hybrid materials*

The IR-spectra of the hybrid materials gained by simultaneous polymerization of the monomers **1** and **2** or **3** or **4** or **5** in different molar ratios are shown in Fig. 4. In the region of 1100 – 950  $\text{cm}^{-1}$  a strong broad band occur through the stretching-vibration of the silica. The O-H-vibration of the phenolic resin occurs in the region of 3500 – 3250  $\text{cm}^{-1}$ . In this region also the N-H-vibration of the aminofunctionalised polysiloxane can be detected for the primary and secondary amines. Due to the superposition of O-H- and N-H-vibration the formation of a doublet for the primary amine cannot be observed. At 1605 and 1590  $\text{cm}^{-1}$  the C=C-vibrations and at 820 and 720  $\text{cm}^{-1}$  the C-H out-of-plane vibration of the aromatic system and the phenolic resin is observable. Latest two bands indicate the formation of ortho and para bonds within the phenolic resin. The doublet of the C=C-vibration is clearly visible in case of high amounts of monomer **1**. The asymmetric and the symmetric C-H stretching vibration of the  $\text{CH}_2$  groups of the methylene bridge within the phenolic resin, as well as of the alkyl chain within the polysiloxane occur in the region 2940 – 2840  $\text{cm}^{-1}$ . In this region also vibrational bands of the  $\text{CH}_3$  groups are observable. The stretching vibration of Si-C of the polysiloxane occurs at 1250  $\text{cm}^{-1}$  (deformation vibration Si- $\text{CH}_3$ ) and at 800  $\text{cm}^{-1}$  (Si-C). At 1250  $\text{cm}^{-1}$  the C-O stretching vibration of the phenolic resin also occurs.

Table 2. Bands of the IR-spectra and the associated vibrations.

wavenumber [cm <sup>-1</sup> ]	vibration
3500 – 3250	$\nu(\text{O-H})$ , C-OH, Si-OH
3600 – 3500	$\nu(\text{N-H})$ , NH <sub>2</sub>
2940 – 2915	$\nu_{\text{as}}(\text{C-H})$ , CH <sub>2</sub> , CH <sub>3</sub>
2870 – 2840	$\nu_{\text{sym}}(\text{C-H})$ , CH <sub>2</sub> , CH <sub>3</sub>
1605, 1590	$\nu(\text{C=C})$ , Aromat
1500, 1450	$\delta_{\text{as}}(\text{C-H})$ , CH <sub>2</sub>
1250	$\delta(\text{Si-CH}_3)$
1100 – 950	$\nu_{\text{as}}(\text{Si-O-Si})$
860	$\delta_{\text{as}}(\text{CH}_3)$
820, 760	$\delta_{\text{out-of-plane}}(\text{CH})$ , Aromat
800	$\nu(\text{Si-C})$

### **Composition of the hybrid materials**

Table 3 show the molecular and the mass distribution of the phenolic resin, silica and the polysiloxane within the hybrid materials. The calculations bases on full conversion of the monomers **1** with **2**, **3**, **4** or **5**.

Table 3. Theoretical content of phenolic resin, silica and polysiloxane in the hybrid materials

Probe	n% Phenolic resin	n% SiO <sub>2</sub>	n% Polysiloxane	m% Phenolic resin	m% SiO <sub>2</sub>	m% Polysiloxane
<b>P2_1</b>	66,1	32,2	1,7	76,4	21,1	2,5
<b>P2_2</b>	64,9	29,8	5,3	73,4	19,1	7,5
<b>P2_3</b>	60,0	20,0	20,0	62,2	11,7	26,1
<b>P2_4</b>	53,5	7,0	39,5	49,9	3,7	46,4
<b>P2_5</b>	50,0	0,0	50,0	44,3	0,0	55,7
<b>P2</b>	60,0	20,0	20,0	62,2	11,7	26,1
<b>P3</b>	60,0	20,0	20,0	60,0	11,1	29,9
<b>P4</b>	60,0	20,0	20,0	60,6	11,4	28,0
<b>P5</b>	60,0	20,0	20,0	57,4	10,8	31,8

Quantitative elemental analysis of the hybrid materials confirm the theoretical composition of the hybrid materials. Table 4 summarize the theoretical content of polysiloxane compared to the real content within the hybrid materials calculated from the nitrogen content determined by quantitative elemental analysis.

Table 4. Theoretical and real content of polysiloxane within the hybrid material calculated from quantitative elemental analysis

Probe	theoretical n% Polysiloxane	N%	calculated n% Polysiloxane
<b>P2_1</b>	1.7	#	*
<b>P2_2</b>	5.3	0.88	5.7
<b>P2_3</b>	20.0	2.81	19.8
<b>P2_4</b>	39.5	5.14	39.0
<b>P2_5</b>	50.0	6.28	50.5
<b>P2</b>	20.0	2.78	20.6
<b>P3</b>	20.0	2.76	20.6
<b>P4</b>	20.0	2.82	20.2
<b>P5</b>	20.0	4.99	18.6

# N-content below detection limit

\* incalculable

### Thermal behavior of the hybrid materials

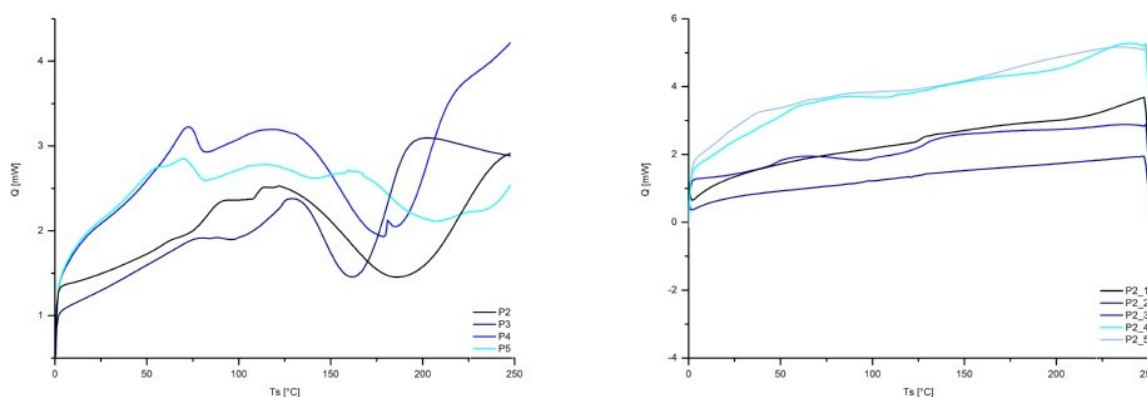


Figure 5. DSC-measurement of the composite Materials **P2**, **P3**, **P4** and **P5** left and **P2\_1**, **P2\_2**, **P2\_3**, **P2\_4** and **P2\_5** right.

The first heating run of the composites **P2**, **P3**, **P4** and **P5**, that have been synthesized at 120 °C show some endothermic peaks between 50 and 80 °C. These might be caused by low molecular weight substances and their melting. Between 100 and 250 °C exothermic peaks appear, that can be associated with post reactions of unreacted Si-O-CH<sub>2</sub> units.

The composite materials **P2\_1**, **P2\_2**, **P2\_3**, **P2\_4** and **P2\_5** which are polymerized at higher temperatures (180 °C) show nearly no endothermic or exothermic peaks within the first heating run of DSC-measurements. Hence, there are no Si-O-CH<sub>2</sub> units which can react during the post heat treatment. These units are also not visible in <sup>13</sup>C-CP-MAS-NMR spectra.

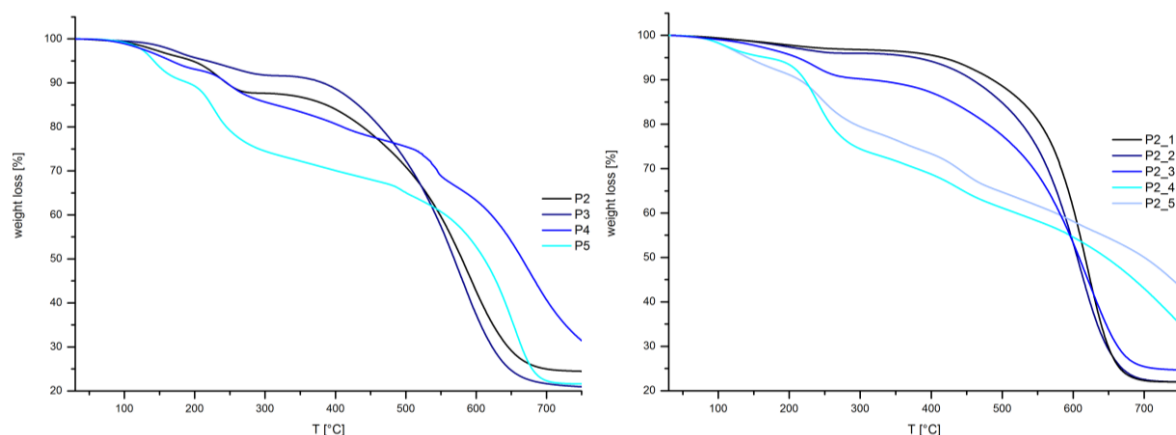


Figure 6. Thermogravimetric analysis of the hybrid materials **P2**, **P3**, **P4**, **P5** (left) and **P2\_1**, **P2\_2**, **P2\_3**, **P2\_4**, **P2\_5** (right).

Figure 6 show the results of the thermogravimetric analysis of the hybrid materials between 30 and 750 °C.

Table 5 summarize the weight loss of the hybrid materials between 30 and 750 °C. Additionally the theoretical weight loss, if all organic compounds (phenolic resin, and CH<sub>3</sub>- and CH<sub>2</sub>CH<sub>2</sub>CH<sub>2</sub>NH<sub>2</sub>-unit of the polysiloxane) of the hybrid material will be oxidized, are added.

Table 5. Theoretical and measured weight loss of the oxidized hybrid materials.

sample	P2	P3	P4	P5	P2_1	P2_2	P2_3	P2_4	P2_5
<b>theoretical</b>									
<b>weight</b>	77.77	77.76	77.17	78.36	77.77	77.52	76.53	75.37	74.88
<b>loss [%]</b>									
<b>weight</b>									
<b>loss [%]</b>	75.52	79.05	68.58	78.39	78.07	78.01	75.30	64.88	56.41
<b>(30-750 °C)</b>									

All samples show a great weight loss between 350 and 750 °C. Most of the samples (**P2**, **P3**, **P5**, **P2\_1**, **P2\_2**, **P2\_2**) were almost completely oxidized till 750 °C. However, samples with a polysiloxane to silica ratio greater than one (**P2\_4**, **P2\_5**) and **P4**, were not fully oxidized till 750 °C.

### **Extraction of the hybrid materials**

All samples have been extracted with DCM for 40h. The weight loss of each sample is listed in table 7. The <sup>1</sup>H-NMR-spectra of the extracted material are shown in figure 7. The spectra show that parts of the phenolic resin and the polysiloxane could be extracted.

Table 6.  $^1\text{H-NMR}$ -signals of the extracted materials

	Signal
Ar-H	7.3 – 6.4
<i>o,o'</i> -CH <sub>2</sub>	4.2 – 3.7
<i>o,p'</i> -CH <sub>2</sub>	
Si-CH <sub>3</sub>	0.4 – 0.0
Si-CH <sub>2</sub> -CH <sub>2</sub> -CH <sub>2</sub> -NH <sub>2</sub>	0.6 – 0.8, 1.4 – 1.6, 2.5 – 2.7
Si-CH <sub>2</sub> -CH <sub>2</sub> -CH <sub>2</sub> -N(CH <sub>3</sub> ) <sub>2</sub>	0.7 – 0.9, 1.5 – 1.7, 2.1 – 2.3, 2.1 – 2.2
Si-CH <sub>2</sub> -CH <sub>2</sub> -CH <sub>2</sub> -NHCH <sub>3</sub>	0.7 – 0.9, 1.5 – 1.7, 2.5 – 2.7, 2.3 – 2.4
Si-CH <sub>2</sub> -CH <sub>2</sub> -CH <sub>2</sub> -NHCH <sub>2</sub> -CH <sub>2</sub> -NH <sub>2</sub>	0.7 – 0.9, 1.5 – 1.7, 2.5 – 2.7, 2.5 – 2.7, 2.7 – 2.9

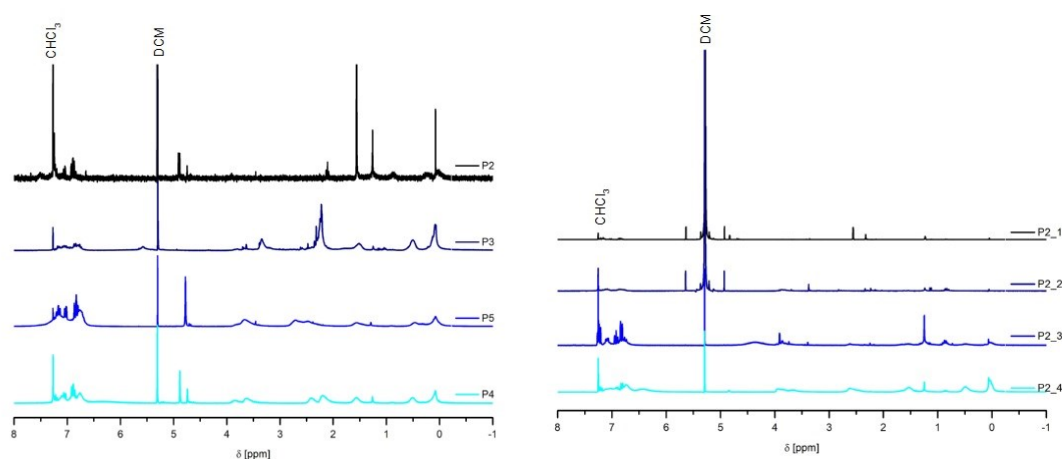


Figure 7.  $^1\text{H-NMR}$ -spectra of the extracted material in  $\text{CDCl}_3$ .

Table 7. Extractable content and GPC data of the extracted material.

run	weight loss [%]	Mw (PD)
<b>P2</b>	42.9	4956 (1.3996), 515 (1.1394), 188 (1.0387), 88 (1.0115)
<b>P3</b>	10.1	867 (1.1796), 326 (1.0188), 195 (1.0263)
<b>P4</b>	58.5	3664 (1.6467), 544 (1.0206), 328 (1.0186), 184 (1.0575)
<b>P5</b>	94.8	2369 (1.2081), 199 (1.0365), 91 (1.0111)
<b>P2_1</b>	0.5	709 (1.1095), 334 (1.0183), 200 (1.0256)
<b>P2_2</b>	1.5	1088 (1.1969), 303 (1.0100), 143 (1.0142)
<b>P2_3</b>	6.1	1002 (1.2748), 329 (1.0379), 136 (1.0382)
<b>P2_4</b>	31.2	928 (1.0905), 329 (1.0092), 146 (1.0282)
<b>P2_5</b>	23.9	360 (1.0198), 144 (1.0213)

## TEM

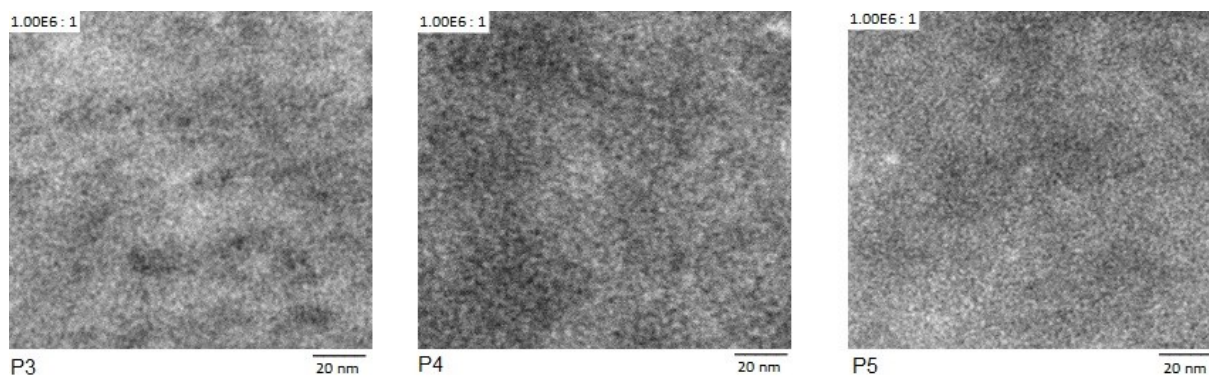


Figure 8. HAADF-STEM images of the composite materials **P3**, **P4** and **P5**.

The HAADF-STEM images of the composite materials show silicon rich domains (bright contrast) with 2-4 nm in size.

## Formation of Schiff-base

The composite material was ground in a steel mill and suspended in toluene. 1.1 eq. (regard to the amino groups) of the aldehyde is added to the suspension. The toluene is removed under reduced pressure and 40 °C. The composite material was suspended again in toluene, in order to wash out unreacted aldehyde, three times.

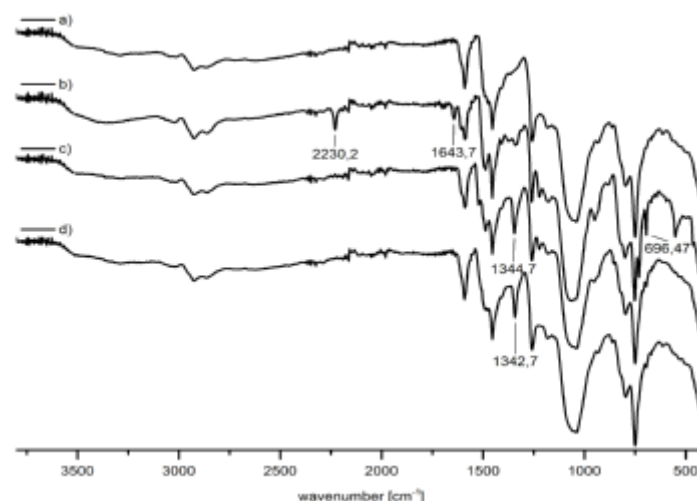


Figure 9. ATR-FTIR-spectra a) of the untreated composite material **P2\_3** and the samples b) **SB1**, c) **SB2** and d) **SB3**.

The conversion of the amino groups was determined by the nitrogen content from elemental analysis by comparing the nitrogen content of the samples with the theoretical nitrogen content, if 100 % of the aminogroups have reacted. These data is listed in table 8.

*Table 8: Nitrogen content and quantity of conversion of the investigated hybrid materials*

run	aldehyde	nitrogen content reference*	calculated nitrogen content for reaction of all amino groups	measured nitrogen content of the sample	conversion
<b>SB1</b>	4-nitrobenzaldehyde	2.96 %	4.61 %	3.29 %	20.3 %
<b>SB2</b>	4-cyanobenzaldehyde	2.96 %	4.76 %	4.16 %	66.7 %
<b>SB3</b>	4-nitrocinnamaldehyde	2.96 %	4.42 %	3.17 %	14.3 %

\* reference has been treated similar without adding any aldehyde

## Literature

- (1) Spange, S.; Kempe, P.; Seifert, A.; Auer, A. A.; Ecorchard, P.; Lang, H.; Falke, M.; Hietschold, M.; Pohlers, A.; Hoyer, W.; Cox, G.; Kockrick, E.; Kaskel, S. *Angew. Chem.* **2009**, *121*, 8403–8408.